Check for updates

Received: 20 June 2021 | Revised: 26 July 2021 | Accepted: 1 September 2021

DOI: 10.1111/jcpe.13546

ORIGINAL ARTICLE

Journal of Clinical Periodontology WILEY

Differences in platelet-rich plasma composition influence bone healing

Faez Saleh Al-Hamed[1] | Lina Abu-Nada[1] | Rania Rodan[1] | Stylianos Sarrigiannidis[2] | Jose Luis Ramirez-Garcialuna[3,4] | Hanan Moussa[1,5] | Osama Elkashty[1,6] | Qiman Gao[1] | Tayebeh Basiri[1] | Laura Baca[7] | Jesus Torres[7] | Lisa Rancan[8] | Simon D. Tran[1] | Marie Lordkipanidzé[9,10] | Mari Kaartinen[1] | Zahi Badran[11,12] | Faleh Tamimi[13]

[1]Faculty of Dentistry, McGill University, Montreal, Canada

[2]Centre for the Cellular Microenvironment, School of Engineering, University of Glasgow, Glasgow, UK

[3]Faculty of Medicine, McGill University, Montreal, Canada

[4]The Bone Engineering Labs, Research Institute McGill University Health Center, Montreal, Canada

[5]Faculty of Dentistry, Benghazi University, Benghazi, Libya

[6]Faculty of Dentistry, Mansoura University, Mansoura, Egypt

[7]Dental Clinical Specialities Department, Faculty of Dentistry, Complutense University, Madrid, Spain

[8]Department of Biochemistry & Molecular Biology, Faculty of Medicine, Complutense University of Madrid, Madrid, Spain

[9]Faculté de Pharmacie, Université de Montréal, Montreal, Canada

[10]Research Center, Montreal Heart Institute, Montreal, Canada

[11]Department of Periodontology (CHU/Rmes Inserm U1229/UIC11), Faculty of Dental Surgery, University of Nantes, Nantes, France

[12]College of Dental Medicine, University of Sharjah, Sharjah, UAE

[13]College of Dental Medicine, Qatar University, Doha, Qatar

Correspondence
Faleh Tamimi, College of Dental Medicine, Qatar University, Building H12 Annex, PO Box 2713, Doha, Qatar.
Email: fmarino@qu.edu.qa

Funding information
Faez Saleh Al-Hamed was supported by a scholarship from Al Awn Foundation for Development, Yemen; Ph.D. training award from Funds de Recherche Québec—Santé (FRQS: 257709); and the Alpha Omega Foundation of Canada grant (2018 and 2019). He also received the Graduate Excellence Award from the Faculty of Dentistry, McGill University. Lina Abu-Nada was supported by Ph.D. training award from Funds de Recherche Québec—Santé and RSBO. Marie Lordkipanidzé is a Canada Research Chair in Platelets as Vectors and Biomarkers. The authors also acknowledge support from the Canada Research Chair Program and Le Réseau de recherche en santé buccodentaire et osseuse (RSBO).

Abstract

Aim: Platelet-rich plasma (PRP) is an autologous blood-derived material that has been used to enhance bone regeneration. Clinical studies, however, reported inconsistent outcomes. This study aimed to assess the effect of changes in leucocyte and PRP (L-PRP) composition on bone defect healing.

Materials and Methods: L-PRPs were prepared using different centrifugation methods and their regenerative potential was assessed in an in-vivo rat model. Bilateral critical-size tibial bone defects were created and filled with single-spin L-PRP, double-spin L-PRP, or filtered L-PRP. Empty defects and defects treated with collagen scaffolds served as controls. Rats were euthanized after 2 weeks, and their tibias were collected and analysed using micro-CT and histology.

Results: Double-spin L-PRP contained higher concentrations of platelets than single-spin L-PRP and filtered L-PRP. Filtration of single-spin L-PRP resulted in lower concentrations of minerals and metabolites. In vivo, double-spin L-PRP improved bone

This is an open access article under the terms of the Creative Commons Attribution-NonCommercial License, which permits use, distribution and reproduction in any medium, provided the original work is properly cited and is not used for commercial purposes.
© 2021 The Authors. *Journal of Clinical Periodontology* published by John Wiley & Sons Ltd.

healing by significantly reducing the size of bone defects (1.08 ± 0.2 mm^3) compared to single-spin L-PRP (1.42 ± 0.27 mm^3) or filtered L-PRP (1.38 ± 0.28 mm^3). There were fewer mast cells, lymphocytes, and macrophages in defects treated with double-spin L-PRP than in those treated with single-spin or filtered L-PRP.

Conclusion: The preparation method of L-PRP affects their composition and potential to regenerate bone.

KEYWORDS

bone formation, bone healing, critical size defect, platelet concentrates, platelet-rich plasma, rat surgery

Clinical Relevance

Scientific rationale for the study: Platelet-rich plasma (PRP) is widely used to enhance bone regeneration in orthopaedic and craniofacial surgeries; however, there are discrepancies in their therapeutic effects.

Principal findings: We have found the extent of healing in bone defects to be directly related to the concentration of platelets in leucocyte and PRP (L-PRP). Double spin L-PRP resulted in better bone healing compared to single-spin or filtered L-PRP.

Practical implications: The use of double-spin L-PRP may enhance their regenerative potential in clinical practice.

1 | INTRODUCTION

Bone fractures represent a major health concern worldwide. Every year, around eight million patients in the United States suffer from bone fractures and may develop further complications such as delayed healing and non-union (Victoria et al., 2009; Yamamoto et al., 2013). Furthermore, pathological bone defects can cause significant morbidity. Different types of bone grafts, including autogenous bone grafts, allografts, xenografts, and alloplasts, as well as biological materials such as platelet concentrates (PCs) have been used to restore bone defects and manage bone fractures (Lawson & Biller, 1982; Albanese et al., 2013; Kumar et al., 2013).

PCs are autologous materials obtained from centrifuged whole blood; they are classified into four main types based on their content of leukocytes and fibrin architecture: pure platelet-rich plasma (P-PRP), leukocyte and platelet-rich plasma (L-PRP), pure platelet-rich fibrin (P-PRF), and leukocyte and platelet-rich fibrin (L-PRF) (Eskan & Greenwell, 2011; Dohan Ehrenfest et al., 2012). P-PRP preparations include plasma rich in growth factors (PRGFs) and activated PRGFs (Fuerst et al., 2004; Eskan & Greenwell, 2011). These materials contain high concentrations of platelets and growth factors (GFs), which are known to enhance osteogenesis, angiogenesis, and tissue regeneration (Al-Hamed et al., 2019). These GFs, which are released from platelet alpha granules, include transforming growth factor beta (TGF-β), fibroblast growth factor, platelet-derived growth factor (PDGF), vascular endothelial growth factor, brain-derived neurotrophic factor, and insulin-like growth factor (IGF) (Masuki et al., 2016). Indeed, in addition to GF-rich alpha granules, platelets express dense granules, which release molecules that could have a negative effect on bone healing, such as serotonin, adenosine triphosphate, and polyphosphate (Badran et al., 2018). Thus, the balance between platelets' pro-osteogenic and anti-osteogenic properties is important in defining the quality of PC preparations.

PCs have been extensively used in dento-alveolar and maxillofacial surgery (Al-Hamed et al., 2017, 2019; Dragonas et al., 2019). PCs have been reported to enhance soft tissue healing and reduce pain and discomfort, but in regard to bone regeneration, there is great heterogeneity in the available studies and limited number of RCTs, which did not lead to any robust conclusion (Donos et al., 2019; Sanz et al., 2019). This could be explained by the differences in study designs and types of PCs (Del Corso et al., 2012; Badran et al., 2018; Harrison, 2018). The concentration of platelets in PCs could play a key role in bone healing. In vitro studies have shown that PCs with a high platelet concentration improved osteoblast proliferation, although these findings have not been confirmed in vivo yet (Kawasumi et al., 2008). Also, it has been hypothesized that the variability in the concentration of platelets and their dense granules could affect their regenerative potential (Badran et al., 2018).

PRP can be prepared using single-spin or double-spin centrifugation protocols. In the former, a blood sample is collected in a tube with an anticoagulant and immediately centrifuged. This short step separates red blood cells (RBCs) from PRP. In the double-spin protocol, whole blood is centrifuged twice, resulting in higher concentrations of platelets in PRPs (El-Husseiny et al., 2020). Furthermore, the use of single-spin and double-spin PRP protocols may produce different concentrations of metabolites and other molecules, which could affect their regenerative potential.

Clinical evidence shows high heterogeneity among different studies in regard to the efficacy of different types of PCs on bone

1600051x, 2021, 12, Downloaded from https://onlinelibrary.wiley.com/doi/10.1111/jcpe.13546 by Spanish Cochrane National Provision (Ministerio de Sanidad), Wiley Online Library on [31/10/2023]. See the Terms and Conditions (https://onlinelibrary.wiley.com/terms-and-conditions) on Wiley Online Library for rules of use; OA articles are governed by the applicable Creative Commons License

regeneration. In addition, different PRP preparation protocols may produce variable concentrations of platelets, metabolites, and other molecules, which could affect their regenerative potential. Therefore, we aimed to investigate how differences in PC composition would influence their ability to regenerate bone. In this study, we chose to test the changes in the composition of PRP but not PRF, as it is unfeasible to modify platelet concentration or to filter small molecules when using PRF because of the formation of the fibrin clot. We first prepared PRP using a single-step centrifugation protocol (single-spin L-PRP) or a two-step protocol (double-spin L-PRP). To assess the effect of L-PRP-derived small molecules and metabolites on bone healing, we developed a new centrifugal filtration protocol using dialysis centrifugal concentrators to produce filtered L-PRP. The regenerative performance of different PRPs was assessed in vivo using a rat model of critical size tibial bone defects.

2 | MATERIALS AND METHODS

This study was approved by the McGill Animal Care and Use Committee (protocol # 2012-7269) in accordance with the Canadian Council for Animal Care guidelines. This study was conducted following ARRIVE guidelines for reporting pre-clinical studies. A total of 35 rats were used in this study, of which 11 were used for L-PRP preparation and the remaining 24 were used for bone defect surgeries.

2.1 | L-PRP preparation and characterization

A total of 11 healthy Sprague Dawley rats were used for L-PRP preparation. Blood samples were collected via cardiac puncture in 10-ml acid citrate dextrose tubes (BD Vacutainer™). From each rat, two samples were collected. The blood retrieved was immediately used to produce three different types of L-PRP as follows: single-spin L-PRP, double-spin L-PRP, and filtered L-PRP. In this study, a centrifuge with a fixed angle rotor (centrifugation radius = 12 cm, Eppendorf 5810R) was used. The centrifugation force (*g*) ranged from 100 to 4000*g* (1092–5460 rpm) (Slichter & Harker, 1976; Perez et al., 2014; Miron et al., 2019). The different plasma samples obtained from different rats were pooled together to eliminate inter-individual differences (such as differences in complete blood count between rats), which made it easier to compare the differences in the preparation protocols (Figure 1).

2.1.1 | Single-spin L-PRP

Blood samples were centrifuged at 160–400*g* for 15 min at room temperature. This process separated blood into two components: the RBCs in the bottom, and the single-spin L-PRP in the top of the centrifugation tube. Then, the RBC layer was discarded and the single-spin PC was collected in a separate tube. A platelet activator ($CaCl_2$, 23 mM) was added prior to surgery to produce an L-PRP gel.

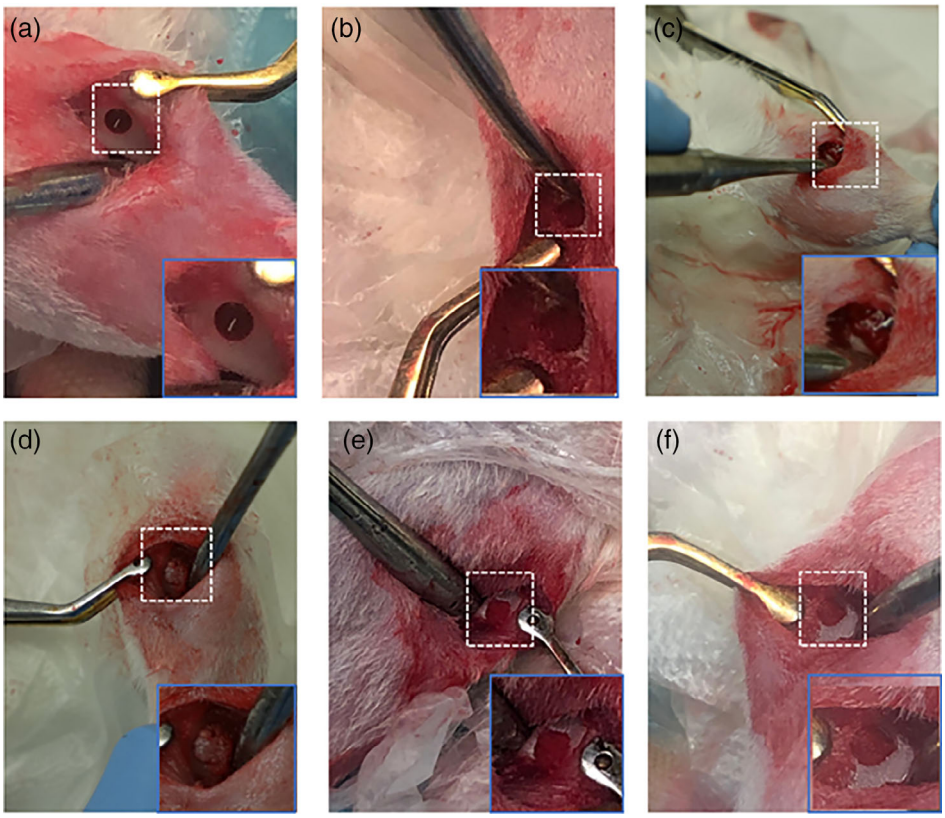

FIGURE 1 Photographs showing bone defect surgery. (a) A unicortical bone defect was created in the lateral surface of tibial metaphysis and left empty as a control. (b) Bone defect filled with single-spin L-PRP. (c) Bone defect filled with double-spin L-PRP. (d) Bone defect filled with filtered L-PRP. (e) Bone defect filled with the collagen scaffold. (f) Bone defect filled with the collagen scaffold and the filtrate material

1600051x, 2021, 12, Downloaded from https://onlinelibrary.wiley.com/doi/10.1111/jcpe.13546 by Spanish Cochrane National Provision (Ministerio de Sanidad), Wiley Online Library on [31/10/2023]. See the Terms and Conditions (https://onlinelibrary.wiley.com/terms-and-conditions) on Wiley Online Library for rules of use; OA articles are governed by the applicable Creative Commons License

2.1.2 | Double-spin L-PRP

The blood samples were centrifuged at 160–400*g* for 15 min at room as described above. Then, the RBC layer was discarded and the platelet-rich plasma was collected in a separate tube. The platelet-rich plasma was then centrifuged at 4000*g* for 30 min. Then the platelet pellet was resuspended in 50% original volume of the plasma to prepare double-spin L-PRP, while the supernatant layer was discarded. The platelet activator ($CaCl_2$, 23 mM) was added prior to surgery to produce an L-PRP gel.

2.1.3 | Filtered L-PRP

This procedure was developed to obtain a similar concentration of platelets as obtained with single-spin L-PRP, while modifying its composition by reducing the concentration of L-PRP metabolites and small molecules. First, single-spin L-PRP was obtained as described above. The platelet activator ($CaCl_2$) was added in order to release the small molecules and allow their removal using the dialysis centrifugal concentrator before the L-PRP clotted. The small molecules and metabolites were removed using a dialysis centrifugal concentrator (Amicon Ultra-15, Millipore, Sigma) with a 3-kDa cut-off. Saline was added to maintain consistent volume and concentration of the platelets.

A range of centrifuging forces (500–4000*g*) and times (5–40 min), as well as volumes of saline (1:1and 1:0.5 ratios) and activator (0 , 3 , and 23 mM), were tested and optimized in order to maintain a constant concentration of platelets while modifying the composition of L-PRP (Figures S1 and S2).

2.1.4 | PRP analysis

Complete blood count was assessed in whole blood, single-spin L-PRP, and double-spin L-PRP using a haematology analyser (SCIL Vet ABC+, Canada). Serotonin concentration in single-spin L-PRP, double-spin L-PRP, filtered L-PRP, and filtrate samples was assessed using a serotonin competitive ELISA kit (Abcam 133053, Canada; Almishri et al., 2019). The elemental compositions of single-spin L-PRP, double-spin L-PRP, filtered L-PRP, and filtrate samples were measured using inductively coupled plasma optical emission spectrometry (Thermo Scientific iCAP 6500, Cambridge, UK) as described previously (Hudson et al., 2015; Al-Hamed et al., 2021). Metabolites of different samples were extracted and analysed based on targeted metabolite analysis using ion-paring liquid chromatography-mass spectrometry or gas chromatography-MS as described previously (Vincent et al., 2015; Al-Hamed et al., 2021).

2.2 | Collagen scaffold preparation

In this study, a collagen scaffold was used as carrier for the filtrate material and as a control. Collagen sponges were prepared as described previously (Varley et al., 2016).

2.3 | In vivo experiments

2.3.1 | Animals

A total of 24 healthy female Sprague Dawley rats (10–12 weeks old; Charles River Laboratories, Montreal, Quebec), weighing 200–250 g were housed (two animals per cage) in the Genome Animal Facility of McGill University. Water and a rodent diet were provided ad libitum, and rats were monitored daily by a veterinarian in the animal facility. Additional seven rats were used for L-PRP preparation as described previously.

2.4 | Bone surgery

To study the effect of single spin L-PRP, double spin L-PRP, filtered L-PRP, and filtrate samples on bone healing, we used a well-established rat tibial critical-size bone defect model (Al Subaie, Laurenti et al., 2016). The bilateral tibial bone defects (2.5 mm diameter, ~2 mm depth) were created in 24 rats as previously described (Al Subaie, Laurenti et al., 2016). Bone defects were randomly divided by using the sealed envelope method into six subgroups in which the following materials were tested for their efficacy to promote bone healing: single-spin L-PRP, double-spin L-PRP, filtered L-PRP, collagen–filtrate scaffold, collagen scaffold, and empty defect (Figures 2 and S3).

Post-operatively, rats were monitored daily, and caprofen (5 mg/kg) was used to control pain for the first 3 days after the surgery. Out of the 24 rats that underwent bone surgeries, 4 were euthanized during the first 3 days due to open wounds and bone fractures and thus were excluded from further analysis. The remaining rats were euthanized after 2 weeks using an overdose of CO_2, and their tibiae were collected and analysed using micro-CT (μ-CT) and histology. The same bone samples used for the μ-CT analyses were also used for histological analyses.

2.5 | Micro-computed tomography

μ-CT analysis was conducted as described previously (Al Subaie, Emami et al., 2016). Briefly, tibiae with bone defects were scanned using a μ-CT apparatus (Sky-Scan1172; Bruker, Kontich, Belgium) set at 12.7 μm resolution, 50 kV voltage, 0.5 rotation step, 10 random movements, and 0.5 mm aluminium filter. The region of interest was defined as the original defect (2.5 mm diameter) and analysed by the CT analyser software (SkyScan; Bruker, Kontich, Belgium). Three-dimensional (3-D) bone parameters were calculated based on the 3-D reconstructed images.

2.6 | Histology and histomorphology

Histology and histomorphology analyses were conducted as previously described (Al-Hamed et al., 2021). The tibias were dehydrated in increasing concentrations of ethanol (70%–100%). Samples were pre-infiltrated with Paraplast X-Tra wax at 58°C and embedded in paraffin

1600051x, 2021, 12, Downloaded from https://onlinelibrary.wiley.com/doi/10.1111/jcpe.13546 by Spanish Cochrane National Provision (Ministerio de Sanidad), Wiley Online Library on [31/10/2023]. See the Terms and Conditions (https://onlinelibrary.wiley.com/terms-and-conditions) on Wiley Online Library for rules of use; OA articles are governed by the applicable Creative Commons License

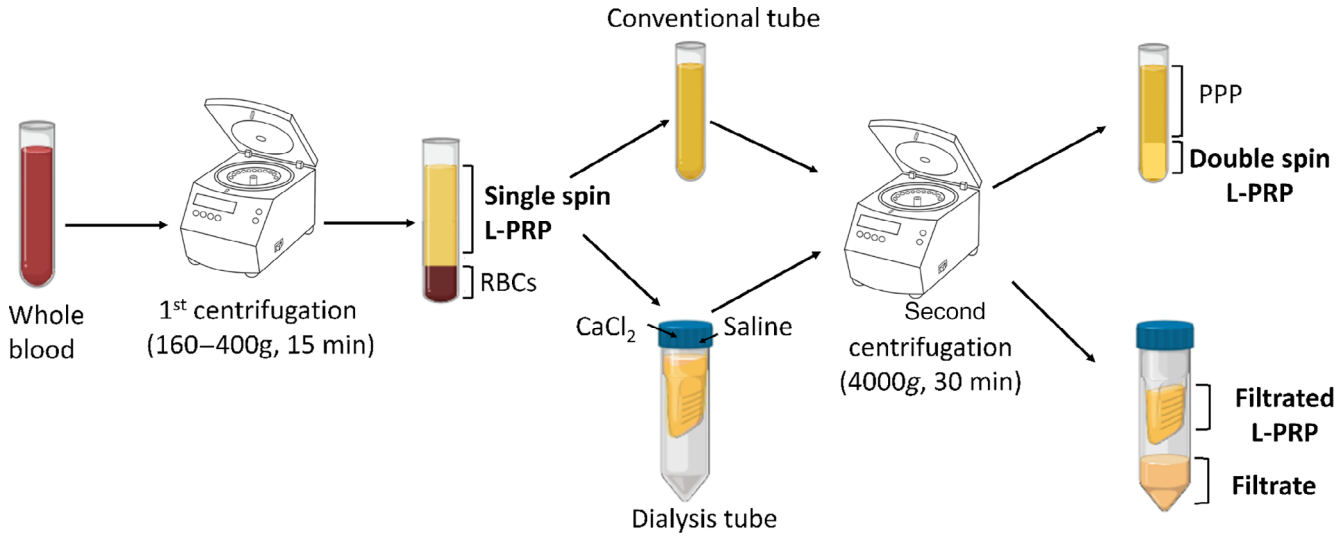

FIGURE 2 Diagram showing the steps followed in the preparation of single-spin L-PRP, double-spin L-PRP, filtered L-PRP, and filtrate samples

wax (EG1160-Leica) and cut into 5-μm-thick sections using a microtome (RM2265-Leica). Five sagittal sections, which included the centre of the defect, were obtained from each bone sample. Sections were stained with tartrate-resistant acid phosphatase (TRAP), haematoxylin and eosin (H&E), and acidified toluidine blue stains to assess the number of osteoclasts, mononuclear immune cells (macrophages and lymphocytes), and mast cells, respectively. Von Kossa stain was used to measure the percentage of new bone formation.

2.7 | Blinding

The retrieved L-PRPs samples and bone samples were anonymously labelled. μ-CT, whole blood count, minerals, and metabolite analyses were performed by a researcher blinded to the group allocation.

2.8 | Statistical analyses

Sample size was calculated based on 95% confidence interval and a statistical power of 80% to be able to reject the null hypothesis that the regenerative ability of different PCs is comparable. Considering a 20% mean change of the defect size to be clinically relevant and assuming a 12% potential standard deviation based on previous studies, a total of six defects were determined to be adequate for each treatment group (Malhotra et al., 2014; Al Subaie, Laurenti et al 2016).

The primary outcome was the defect size (measured in mm^3). The secondary outcomes were bone volume/tissue volume (BV/TV), cortical thickness, trabecular thickness, trabecular number, and trabecular separation. Normality of data was tested using the Shapiro–Wilk test. ANOVA was used when the data was normally distributed, and the non-parametric Kruskal–Wallis test was used otherwise. In comparisons of two groups, paired-sample *t*-test was used for related samples and unpaired *t*-test for independent samples when data was normally distributed, while the non-parametric Mann–Whitney test was used otherwise. All results are shown as mean ± SD. Values were considered statistically significant at $p < .05$.

3 | RESULTS

3.1 | Compositional differences in PCs

The main characteristics of L-PRPs obtained by single-spin, double-spin, and filtration are presented in Table 1 and Figure 3. As expected, double-spin L-PRP had higher platelet concentrations (3162 ± 1179 × 10^9/L) in comparison with single-spin L-PRP (1077 ± 134 × 10^9/L) and whole blood (632 ± 146 × 10^9/L). Filtration of single-spin L-PRP did not alter significantly the platelet counts and the levels of Fe, P, Zn, and Ni as compared with single-spin L-PRP. However, filtrated L-PRP had significantly decreased levels of Cu, K, Mg, Na, Se, and serotonin and increased levels of Ca than single-spin PC. Double-spin L-PRPs were comparable to single-spin L-PRPs in terms of their elemental levels, except for the higher levels of P and Se, and serotonin.

Metabolite analysis showed a decrease in the relative concentration of metabolites in filtered L-PRP and filtrate samples such as nucleosides, citric acid cycle intermediates, pentose phosphate pathway (PPP), and water-soluble oxidative stress indicators (except glutathione) compared to single- or double-spin L-PRPs.

3.2 | Effect of different types of L-PRPs on bone healing

μ-CT analysis showed that bone defects treated with double-spin L-PRP presented with smaller defect sizes (1.08 ± 0.2 mm^3) compared to defects treated with filtered L-PRP (1.38 ± 0.28 mm^3, $p = .03$) or single-spin L-PRP (1.42 ± 0.27 mm^3, $p = .04$), whereas non-significant

1600051x, 2021, 12, Downloaded from https://onlinelibrary.wiley.com/doi/10.1111/jcpe.13546 by Spanish Cochrane National Provision (Ministerio de Sanidad), Wiley Online Library on [31/10/2023]. See the Terms and Conditions (https://onlinelibrary.wiley.com/terms-and-conditions) on Wiley Online Library for rules of use; OA articles are governed by the applicable Creative Commons License

Composition	Whole blood Mean ± SD	Single-spin L-PRP Mean ± SD	Double-spin L-PRP Mean ± SD	*p* value
Platelets × 10^9/L	632 ± 146	1077 ± 134	3162 ± 1179	<.001
WBCs × 10^9 /L	3.93 ± 1.66	0.81 ± 0.65	2.00 ± 0.00	.11
RBCs ×10^{12}/L	5.65 ± 0.58	0.22 ± 0.23	0.39 ± 0.06	.18

TABLE 1 Complete blood count of whole blood and different L-PRPs

Abbreviations: CBC, complete blood count; WBC, white blood cell; RBC, red blood cell.

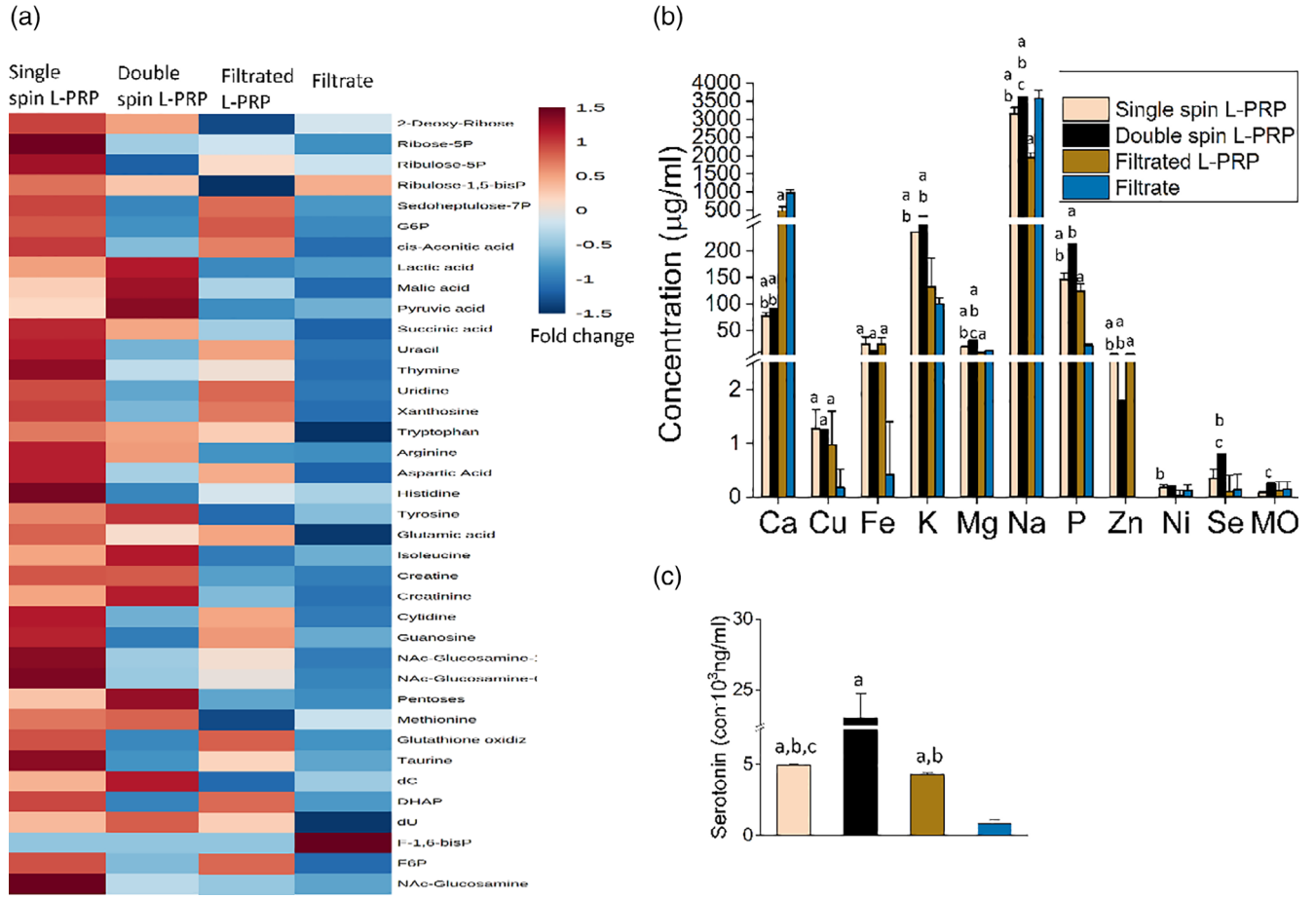

FIGURE 3 PC composition analysis. (a) Hierarchical clustering heatmap showing the fold changes in the levels of selected metabolites measured in single-spin L-PRP, double-spin L-PRP, filtered L-PRP, and filtrate. Red colour indicates high concentration, while blue colour indicates low concentration. (b) Concentration of chemical elements. (c) Serotonin level. The letter "a" indicates significant difference compared to filtrate, the letter "b" indicates significant difference compared to compared to filtered L-PRP, and the letter "c" indicates significant difference compared to single-spin L-PRP

compared to empty defects (1.33 ± 0.42 mm^3, $p = .4$). Also, defects treated with double spin L-PRP showed higher trabecular number (Tb. N, $p = .045$) and lower trabecular separation (Tb.Sp, $p = .030$) compared to empty defects (Figures 4 and 5).

3.2.1 | Histology and histomorphometry

Histological and histomorphological analyses (Figure 6) showed that defects treated with single-spin L-PRP (4.1 ± 1.8 × 10^3 cells/mm^2), filtrated L-PRP (4.2 ± 1.1 × 10^3 cells/mm^2), collagen–filtrate combination (4.9 ± 1.6 × 10^3 cell/mm^2), or collagen alone (3.7 ± 1.9 × 10^3 cells/mm^2) had comparable macrophage and lymphocyte infiltration compared to empty defects (6.3 ± 1.1 × 10^3cells/mm^2, $p > .05$), whereas double-spin L-PRP presented lower numbers of macrophages and lymphocytes (3.4 ± 1.0 × 10^3 cells/mm^2, $p = .01$).

The percentage of mineralized bone in filtered L-PRP (43 ± 10%), single-spin PC (44 ± 7%), and double-spin L-PRP (48 ± 5%) was similar to that of empty defects (43 ± 5%) but higher than that of collagen–filtrate combination (29 ± 11%, $p = .03$, .04, and .01, respectively) or collagen alone (27 ± 16%, $p = .049$, .08, and .03, respectively).

1600051x, 2021, 12, Downloaded from https://onlinelibrary.wiley.com/doi/10.1111/jcpe.13546 by Spanish Cochrane National Provision (Ministerio de Sanidad), Wiley Online Library on [31/10/2023]. See the Terms and Conditions (https://onlinelibrary.wiley.com/terms-and-conditions) on Wiley Online Library for rules of use; OA articles are governed by the applicable Creative Commons License

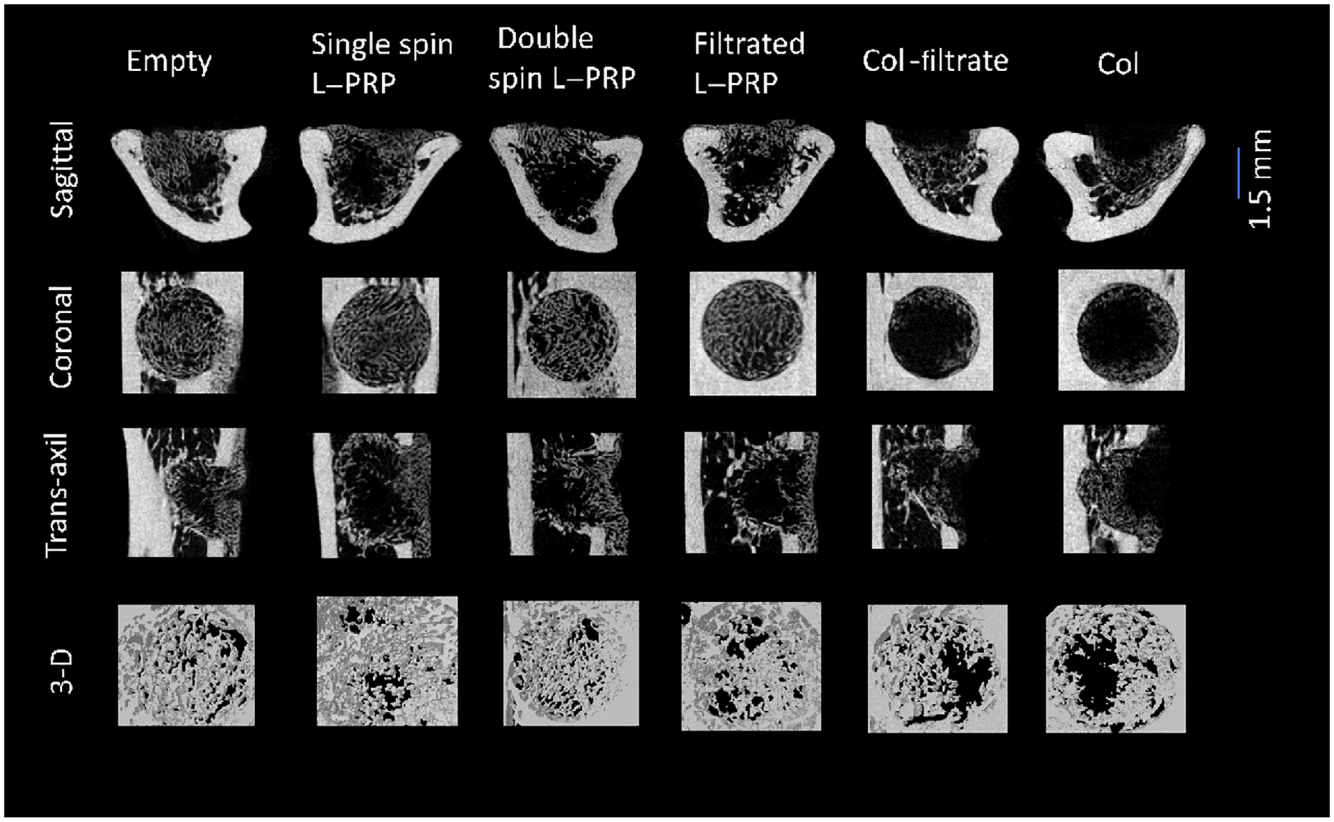

FIGURE 4 Sagittal, coronal, trans-axial, and 3-D μ-CT images of bone defects showing impaired bone healing in defects treated with collagen–filtrate composite and collagen alone compared to other treatment groups. Defects treated with double-spin L-PRP showed reduced defect volume compared to other treatment groups

Mast cell infiltration was significantly higher in filtered L-PRP (165 ± 111 cells/mm^2) and single-spin L-PRP (84 ± 7 cells/mm^2) compared to double-spin L-PRP (20 ± 2 cells/mm^2, $p = .007$ and .001, respectively), or empty defect (34 ± 4 cells/mm^2, $p = .040$ and .001, respectively). Furthermore, the collagen–filtrate composite presented higher mast cell infiltration compared to collagen alone (86 ± 4 vs. 29 ± 5 cells/mm^2, $p = .003$).

4 | DISCUSSION

This is the first study to assess the effect of different L-PRP compositions on bone healing while controlling for inter-individual variability by using head-to-head comparisons of various L-PRPs obtained from the same animals. Taken together, our results suggest that increased platelet concentration in PRP enhances the healing of bone defects, while variations in the concentrations of metabolites do not appear to correlate with the healing potential.

As expected, in the present study double-spin L-PRP had a higher concentration of platelets than single-spin L-PRP and filtered L-PRP, which is in agreement with previous studies (Nagata et al., 2010; Mazzocca et al., 2012). Such an increase in platelet concentration could explain the better bone regeneration observed in defects treated with double-spin L-PRP. In agreement of our findings, it has been reported that a medium concentration of platelets (2.65 $\times$ 10^9 ± 0.2 $\times$ 10^9/ml), which was obtained in the current study by using double-spin L-PRP, promoted osteoblast proliferation, and high concentrations of platelets (8.21 $\times$ 10^9 ± 0.4 $\times$ 10^9/ml) inhibited osteogenic proliferation, whereas a low concentration (0.85 $\times$ 10^9 ± 0.16 $\times$10^9/ml), which was obtained by using single-spin L-PRP and filtered L-PRP, had no effect on osteogenesis (Kawasumi et al., 2008; Chen et al., 2013).

Bone regenerated with double-spin L-PRP presented lower trabecular separation and higher trabecular numbers compared to non-treated defects, which is in agreement with other studies showing that it also improves the trabecular pattern and reduces trabecular separation in humans and animals, respectively (Alissa et al., 2010; Huang et al., 2019). Also, the size of defects treated with double-spin L-PRP was significantly reduced compared to defects treated with single-spin or filtered L-PRP, but not compared to empty defects. The reduction in the defect size was around 0.4 mm^3, which was statistically significant compared to defects treated with single-spin L-PRP or filtered L-PRP. However, the small difference in the defect size seems to be less clinically relevant. These positive effects could be explained by the rich content of L-PRP-derived regenerative proteins such as GFs (e.g., PDGF, TGF, IGF, and bone morphogenic proteins), which are known to enhance osteoblast activity and consequently result in more trabeculae and less separation (Ferreira et al., 2005; Steller et al., 2019).

Our results showed that filtered L-PRP and filtrate samples had lower concentration of metabolites critical to the citric acid cycle, PPP, and nucleotides compared to single- or double-spin L-PRPs. Such

1600051x, 2021, 12, Downloaded from https://onlinelibrary.wiley.com/doi/10.1111/jcpe.13546 by Spanish Cochrane National Provision (Ministerio de Sanidad), Wiley Online Library on [31/10/2023]. See the Terms and Conditions (https://onlinelibrary.wiley.com/terms-and-conditions) on Wiley Online Library for rules of use; OA articles are governed by the applicable Creative Commons License

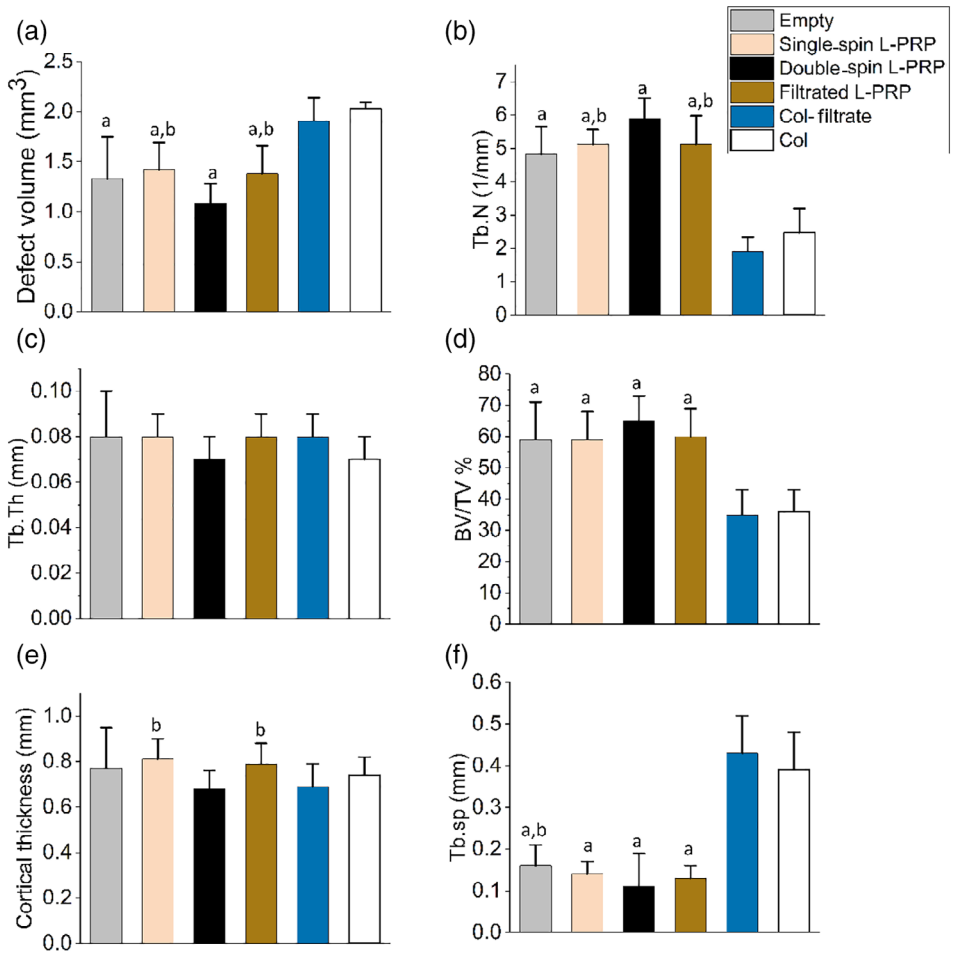

FIGURE 5 Micro-CT data analysis of bone defects treated with different treatments for the following parameters: (a) defect volume, (b) trabecular number (Tb.N), (c) trabecular thickness (Tb.Th), (d) bone volume/tissue volume (BV/TV), (e) cortical thickness, and (f) trabecular separation (Tb.Sp). The letter "a" indicates significant difference compared to collagen groups. The letter "b" indicates significant difference compared to double-spin L-PRP

differences are due to the use of the filter and adding saline and $CaCl_2$ to the filtrate samples prior to the second centrifugation. The citric acid cycle is a key metabolic pathway for body energy supply (Akram, 2014). The PPP is an essential component of cellular metabolism, which maintains carbon homeostasis and anabolism, and provides precursors for nucleotide and amino acids (Stincone et al., 2015).

Our results showed that collagen scaffolds interfere with bone defect healing and that adding the filtrate material did not modify their effect on bone healing. These results could be explained by the slow degradation of collagen scaffolds, which could be attributed to a high degree of cross-linking. Furthermore, the reduced mechanical strength and osteoinductive potential of collagen scaffolds limit their applications for bone regeneration procedures (Zhang et al., 2018). In agreement with our results, the implantation of collagen scaffold in rats did not induce bone formation, whereas the incorporation of bioactive glass into collagen scaffolds has been found to improve scaffold bioactivity and osteogenesis (Zhang et al., 2018).

Our histomorphology results showed comparable inflammatory cell infiltration between defects treated with the collagen–filtrate composite and collagen alone except mast cell infiltration, which was significantly increased in the composite. Mast cells have been identified as regulatory elements of inflammation and bone turnover during bone healing and their numbers are modified by changes in the inflammatory environment (Ramirez-GarciaLuna et al., 2017; Ramirez-Garcia-Luna et al., 2019). Also, mast cell infiltration has been found to be significantly higher in defects treated with single-spin L-PRP and filtered L-PRP compared to empty defects. During early inflammatory reaction, mast cells migrate to the injured site via chemotactic inflammatory signals, and their recruitment is increased by the presence of other materials such as PCs (Ibrahim et al., 2017). Taken together, these findings suggest that the quantity and activity of mast cells are influenced by the PRP composition.

In the present study, the regenerative potential of different types of PRP was assessed using a rat model with tibial bone defect. This model involves minimally invasive surgery and reduces animal suffering. We have already used it in our previous studies with minimal complications (Al-Hamed et al., 2020; Al-Hamed et al., 2021). However, in the current study, our rats were euthanized because of bone fractures. This occurred because of misplacement of the drilled defect, which weakened the bone and thus led to bone fracture.

Overall, the application of different L-PRPs showed non-significant differences in regard to defect volume and BV/TV compared to empty defects (control group). This could be due to the fact that this study was performed in a young group of rats that had high regenerative ability as well as because the tested groups were assessed within the same animal. This may mask the real effect of L-PRP compared to controls. Also, due to the small sample size, we might not have seen the differences in healing between L-PRP and controls. Therefore, further studies with

1600051x, 2021, 12, Downloaded from https://onlinelibrary.wiley.com/doi/10.1111/jcpe.13546 by Spanish Cochrane National Provision (Ministerio de Sanidad), Wiley Online Library on [31/10/2023]. See the Terms and Conditions (https://onlinelibrary.wiley.com/terms-and-conditions) on Wiley Online Library for rules of use; OA articles are governed by the applicable Creative Commons License

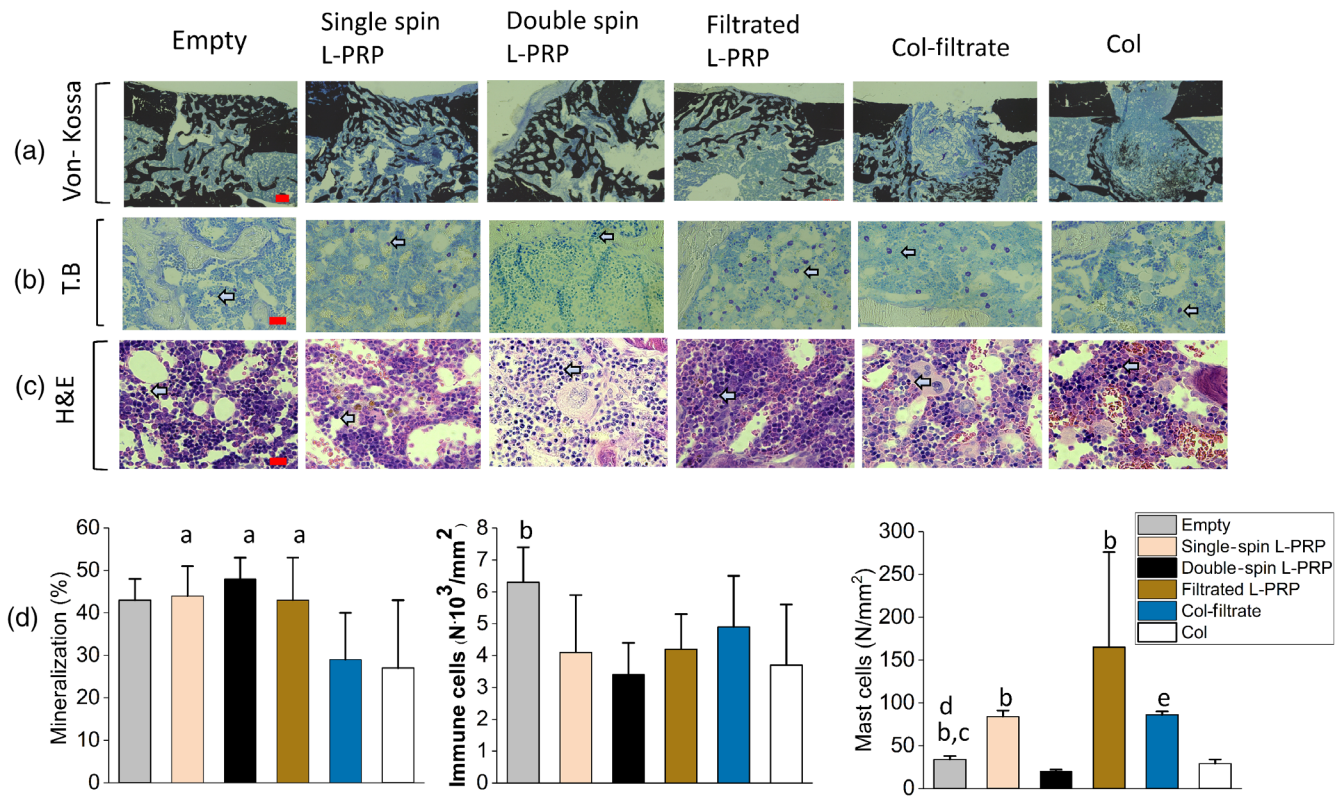

FIGURE 6 Histological and histomorphometric analysis of bone defects obtained from rats received different treatments. (a) Histological cross-sections stained with Von Kossa to assess mineralization % (scale bar = 200 μm). (b) Histological cross-sections of bone samples stained with toluidine blue for mast cell quantification (scale bar = 20 μm). (d) Histological cross-sections of bone samples stained with H&E to assess immune cell infiltration (scale bar = 20 μm). Arrows indicate the cells of interest. (d) Bar charts represent histomorphometric analyses. Data presented as mean ± SD. The letter "a" indicates significant difference compared to collagen groups. The letter "b" indicates significant difference compared to double spin L-PRP. The letter "c" indicates significant difference compared to single-spin L-PRP. The letter "d" indicates significant difference compared to filtered L-PRP. The letter "e" indicates significant difference compared to collagen alone

larger sample sizes are required. Furthermore, the comparable healing observed in empty defects raises a concern regarding the suitability of this bone defect model. However, this model was found to be reliable to study the effect of medications on bone healing based on previous studies (Al Subaie, Laurenti et al. 2016; Al-Hamed et al., 2020). Therefore, to assess the regenerative potential of L-PRP, it is advised to use a larger bone defect instead of the one used in this study.

4.1 | Strengths, limitations, and future directions

This study was the first to show the effect of changes in L-PRP composition on bone healing by understanding the differences between single-spin L-PRP, double-spin L-PRP, and filtered L-PRP, as well as their bone regenerative potential. The main limitation of this study was that the effects of L-PRPs on bone healing were assessed only at one time point, namely 2 weeks after surgery. This time point was selected because it allows accurate assessment of the early stages of bone healing in terms of osteoblastic activity induced by medications or biological materials as reported in our previous studies (Al Subaie, Laurenti et al. 2016; Al-Hamed et al., 2020, 2021). Furthermore, assessing bone healing at shorter time points (<1 week) does not show anything on μ-CT because there is no mineralization yet, and longer time points do not show differences because the defect is completely healed, as we performed the experiment in a group of young rats which have rapid healing ability. However, further studies will be needed to study the long-term plasma effect on bone healing. Also, in this study, we assessed the effect of composition changes of PRPs on bone healing but not soft tissue healing. Therefore, further studies are required to study the effect of changes in PRP composition on soft tissue healing.

5 | CONCLUSION

Changes in the compositional components of L-PRPs affect their potential to regenerate bone. High platelet concentration enhanced the healing of bone defects. Adding the filtrate material to collagen scaffolds did not modify their effect on bone healing.

ACKNOWLEDGEMENTS

The authors would like to thank Dr Tamimi's writing group members for revising the manuscript. They would also like to thank Dr Marc McKee,

1600051x, 2021, 12, Downloaded from https://onlinelibrary.wiley.com/doi/10.1111/jcpe.13546 by Spanish Cochrane National Provision (Ministerio de Sanidad), Wiley Online Library on [31/10/2023]. See the Terms and Conditions (https://onlinelibrary.wiley.com/terms-and-conditions) on Wiley Online Library for rules of use; OA articles are governed by the applicable Creative Commons License

Aisha Mousa, and the Proteomics, Metabolomics, and Histopathology Centres at MUHC for their help in PRP preparation and data analyses.

CONFLICT OF INTEREST

The authors declare no conflict of interest.

AUTHOR CONTRIBUTIONS

Faez Saleh Al-Hamed wrote the manuscript, contributed to the study design, performed bone surgeries, performed the μ-CT scan and analyses, prepared all figures, and carried out statistical analysis and histological assessment of Von Kossa, TRAP, and ALP stained bone samples. Lina Abu-Nada assisted in μ-CT analysis and literature review. Rania Rodan helped in plasma preparation and serotonin analysis. Stylianos Sarrigiannidis prepared collagen scaffolds and revised the manuscript. Jose Luis Ramirez-Garcialuna performed histological assessment of mast cell infiltration. Osama Elkashty performed histological assessment of immune cell infiltration. Hanan Moussa helped in bone surgery experiments. Qiman Gao helped in bone surgery. Tayebeh Basiri helped in ELISA analysis. Laura Baca, Jesus Torres, and Lisa Rancan performed the serotonin release experiment. Simon D. Tran revised the manuscript, Marie Lordkipanidzé and Mari Kaartinen contributed to the study design, revised, and edited the manuscript. Zahi Badran and Faleh Tamimi contributed to the study design and interpretation, edited, and revised the manuscript. All authors approved the final version of the manuscript.

DATA AVAILABILITY STATEMENT

The data that supports the findings of this study are available in the supplementary material of this article

ORCID

Faez Saleh Al-Hamed https://orcid.org/0000-0002-9451-0452
Lina Abu-Nada https://orcid.org/0000-0001-9815-6393
Faleh Tamimi https://orcid.org/0000-0002-4618-8374

REFERENCES

Akram, M. (2014). Citric acid cycle and role of its intermediates in metabolism. *Cell Biochemistry and Biophysics*, *68*(3), 475–478. https://doi.org/10.1007/s12013-013-9750-1

Al-Hamed, F. S., Mahri, M., Al-Waeli, H., Torres, J., Badran, Z., & Tamimi, F. (2019). Regenerative effect of platelet concentrates in oral and craniofacial regeneration. *Frontiers in Cardiovascular Medicine*, *6*, 126. https://doi.org/10.3389/fcvm.2019.00126

Al-Hamed, F. S., Maria, O. M., Phan, J., Al-Subaie, A., Gao, Q., Mansour, A., Nada, L. A., Boukhatem, I., Elkashty, O. A., Tran, S. D., Lordkipanidzé, M., Badran, Z., Tamimi, F., & Tamimi, F. (2020). Postoperative administration of the acetylcholinesterase inhibitor, donepezil, interferes with bone healing and implant osseointegration in a rat model. *Biomolecules*, *10*(9), 1318. Retrieved from. https://www.mdpi.com/2218-273X/10/9/1318

Al-Hamed, F. S., Rodan, R., Ramirez-Garcialuna, J. L., Elkashty, O., Al-Shahrani, N., Tran, S. D., Lordkipanidzé, M., Kaartinen, M., Badran, Z., & Tamimi, F. (2021). The effect of aging on the bone healing properties of blood plasma. *Injury*, *52*(7), 1697–1708. https://doi.org/10.1016/j.injury.2021.05.001

Al-Hamed, F. S., Tawfik, M. A., Abdelfadil, E., & Al-Saleh, M. A. Q. (2017). Efficacy of platelet-rich fibrin after mandibular third molar extraction: A systematic review and meta-analysis. *Journal of Oral and Maxillofacial Surgery*, *75*(6), 1124–1135. https://doi.org/10.1016/j.joms.2017.01.022

Al-Subaie, A. E., Laurenti, M., Abdallah, M. N., Tamimi, I., Yaghoubi, F., Eimar, H., Makhoul, N., & Tamimi, F. (2016). Propranolol enhances bone healing and implant osseointegration in rats tibiae. *Journal of Clinical Periodontology*, *43*(12), 1160–1170. https://doi.org/10.1111/jcpe.12632

Al-Subaie, A., Emami, E., Tamimi, I., Laurenti, M., Eimar, H., Abdallah, M.-N., & Tamimi, F. (2016). Systemic administration of omeprazole interferes with bone healing and implant osseointegration: An in vivo study on rat tibiae. *Journal of Clinical Periodontology*, *43*(2), 193–203. https://doi.org/10.1111/jcpe.12506

Albanese, A., Licata, M. E., Polizzi, B., & Campisi, G. (2013). Platelet-rich plasma (PRP) in dental and oral surgery: From the wound healing to bone regeneration. *Immunity & Ageing*, *10*(1), 23. https://doi.org/10.1186/1742-4933-10-23

Alissa, R., Esposito, M., Horner, K., & Oliver, R. (2010). The influence of platelet-rich plasma on the healing of extraction sockets: An explorative randomised clinical trial. *European Journal of Oral Implantology*, *3*(2), 121–134.

Almishri, W., Shaheen, A. A., Sharkey, K. A., & Swain, M. G. (2019). The antidepressant mirtazapine inhibits hepatic innate immune networks to attenuate immune-mediated liver injury in mice. *Frontiers in Immunology*, *10*, 803. https://doi.org/10.3389/fimmu.2019.00803

Badran, Z., Abdallah, M. N., Torres, J., & Tamimi, F. (2018). Platelet concentrates for bone regeneration: Current evidence and future challenges. *Platelets*, *29*(2), 105–112. https://doi.org/10.1080/09537104.2017.1327656

Chen, L., Yang, X., Huang, G., Song, D., Ye, X. S., Xu, H., & Li, W. (2013). Platelet-rich plasma promotes healing of osteoporotic fractures. *Orthopedics*, *36*(6), e687–e694. https://doi.org/10.3928/01477447-20130523-10

Del Corso, M., Vervelle, A., Simonpieri, A., Jimbo, R., Inchingolo, F., Sammartino, G., & Dohan Ehrenfest, D. M. (2012). Current knowledge and perspectives for the use of platelet-rich plasma (PRP) and platelet-rich fibrin (PRF) in oral and maxillofacial surgery part 1: Periodontal and dentoalveolar surgery. *Current Pharmaceutical Biotechnology*, *13*(7), 1207–1230.

Dohan Ehrenfest, D. M., Bielecki, T., Mishra, A., Borzini, P., Inchingolo, F., Sammartino, G., Rasmusson, L., & Everts, P. A. (2012). In search of a consensus terminology in the field of platelet concentrates for surgical use: Platelet-rich plasma (PRP), platelet-rich fibrin (PRF), fibrin gel polymerization and leukocytes. *Current Pharmaceutical Biotechnology*, *13*(7), 1131–1137. https://doi.org/10.2174/138920112800624328

Donos, N., Dereka, X., & Calciolari, E. (2019). The use of bioactive factors to enhance bone regeneration: A narrative review. *Journal of Clinical Periodontology*, *46*(S21), 124–161. https://doi.org/10.1111/jcpe.13048

Dragonas, P., Schiavo, J. H., Avila-Ortiz, G., Palaiologou, A., & Katsaros, T. (2019). Plasma rich in growth factors (PRGF) in intraoral bone grafting procedures: A systematic review. *Journal of Cranio-Maxillo-Facial Surgery*, *47*(3), 443–453. https://doi.org/10.1016/j.jcms.2019.01.012

El-Husseiny, R. M., Saleh, H. M., Moustafa, A. A., & Salem, S. A. (2020). Comparison between single- versus double-spin prepared platelet-rich plasma injection in treatment of female pattern hair loss: Clinical effect and relation to vascular endothelial growth factor. *Archives of Dermatological Research*, *313*, 557–566. https://doi.org/10.1007/s00403-020-02134-6

Eskan, M. A., & Greenwell, H. (2011). Theoretical and clinical considerations for autologous blood preparations: Platelet-rich plasma, fibrin sealants, and plasma-rich growth factors. *Clinical Advances in Periodontics*, *1*(2), 142–153. https://doi.org/10.1902/cap.2011.110034

Ferreira, C. F., Carriel Gomes, M. C., Filho, J. S., Granjeiro, J. M., Oliveira Simoes, C. M., & Magini Rde, S. (2005). Platelet-rich plasma influence on human osteoblasts growth. *Clinical Oral Implants Research*, *16*(4), 456–460. https://doi.org/10.1111/j.1600-0501.2005.01145.x

Fuerst, G., Reinhard, G., Tangl, S., Mittlböck, M., Sanroman, F., & Watzek, G. (2004). Effect of platelet-released growth factors and collagen type I on osseous regeneration of mandibular defects. *Journal of Clinical Periodontology*, *31*(9), 784–790. https://doi.org/10.1111/j.1600-051X.2004.00561.x

1600051x, 2021, 12, Downloaded from https://onlinelibrary.wiley.com/doi/10.1111/jcpe.13546 by Spanish Cochrane National Provision (Ministerio de Sanidad), Wiley Online Library on [31/10/2023]. See the Terms and Conditions (https://onlinelibrary.wiley.com/terms-and-conditions) on Wiley Online Library for rules of use; OA articles are governed by the applicable Creative Commons License

Harrison, P. (2018). The use of platelets in regenerative medicine and proposal for a new classification system: Guidance from the SSC of the ISTH. *Journal of Thrombosis and Haemostasis*, *16*(9), 1895–1900. https://doi.org/10.1111/jth.14223

Huang, Y., Li, Z., Van Dessel, J., Salmon, B., Huang, B., Lambrichts, I., Politis, C., & Jacobs, R. (2019). Effect of platelet-rich plasma on peri-implant trabecular bone volume and architecture: A preclinical micro-CT study in beagle dogs. *Clinical Oral Implants Research*, *30*(12), 1190–1199. https://doi.org/10.1111/clr.13532

Hudson, R., Chazelle, V., Bateman, M., Roy, R., Li, C.-J., & Moores, A. (2015). Sustainable synthesis of magnetic ruthenium-coated iron nanoparticles and application in the catalytic transfer hydrogenation of ketones. *ACS Sustainable Chemistry & Engineering*, *3*(5), 814–820. https://doi.org/10.1021/acssuschemeng.5b00206

Ibrahim, M., Bond, J., Medina, M. A., Chen, L., Quiles, C., Kokosis, G., Bashirov, L., Klitzman, B., & Levinson, H. (2017). Characterization of the foreign body response to common surgical biomaterials in a murine model. *European Journal of Plastic Surgery*, *40*(5), 383–392. https://doi.org/10.1007/s00238-017-1308-9

Kawasumi, M., Kitoh, H., Siwicka, K. A., & Ishiguro, N. (2008). The effect of the platelet concentration in platelet-rich plasma gel on the regeneration of bone. *Journal of Bone and Joint Surgery. British Volume (London)*, *90*(7), 966–972. https://doi.org/10.1302/0301-620x.90b7.20235

Kumar, P., Vinitha, B., & Fathima, G. (2013). Bone grafts in dentistry. *Journal of Pharmacy and Bioallied Sciences*, *5*(5), 125–127. https://doi.org/10.4103/0975-7406.113312

Lawson, W., & Biller, H. F. (1982). Mandibular reconstruction: Bone graft techniques. *Otolaryngology and Head and Neck Surgery*, *90*(5), 589–594. https://doi.org/10.1177/019459988209000514

Malhotra, A., Pelletier, M. H., Yu, Y., Christou, C., & Walsh, W. R. (2014). A sheep model for cancellous bone healing. *Frontiers in Surgery*, *1*(37), 1–7. https://doi.org/10.3389/fsurg.2014.00037

Masuki, H., Okudera, T., Watanebe, T., Suzuki, M., Nishiyama, K., Okudera, H., Nakata, K., Uematsu, K., Su, C.-Y., & Kawase, T. (2016). Growth factor and pro-inflammatory cytokine contents in platelet-rich plasma (PRP), plasma rich in growth factors (PRGF), advanced platelet-rich fibrin (A-PRF), and concentrated growth factors (CGF). *Int J Implant Dent*, *2*(1), 19. https://doi.org/10.1186/s40729-016-0052-4

Mazzocca, A. D., McCarthy, M. B., Chowaniec, D. M., Cote, M. P., Romeo, A. A., Bradley, J. P., Arciero, R. A., & Beitzel, K. (2012). Platelet-rich plasma differs according to preparation method and human variability. *The Journal of Bone and Joint Surgery. American Volume*, *94*(4), 308–316. https://doi.org/10.2106/jbjs.K.00430

Miron, R. J., Pinto, N. R., Quirynen, M., & Ghanaati, S. (2019). Standardization of relative centrifugal forces in studies related to platelet-rich fibrin. *Journal of Periodontology*, *90*(8), 817–820. https://doi.org/10.1002/jper.18-0553

Nagata, M. J. H., Messora, M. R., Furlaneto, F. A. C., Fucini, S. E., Bosco, A. F., Garcia, V. G., Deliberador, T. M., & de Melo, L. G. N. (2010). Effectiveness of two methods for preparation of autologous platelet-rich plasma: An experimental study in rabbits. *European Journal of Dentistry*, *4*(4), 395–402. Retrieved from. https://pubmed.ncbi.nlm.nih.gov/20922159, https://www.ncbi.nlm.nih.gov/pmc/articles/PMC2948740/

Perez, A. G., Lana, J. F. S., Rodrigues, A. A., Luzo, A. C. M., Belangero, W. D., & Santana, M. H. A. (2014). Relevant aspects of centrifugation step in the preparation of platelet-rich plasma. *International Scholarly Research Notices*, *2014*(4), 176060.

Ramirez-Garcia-Luna, J. L., Wong, T. H., Chan, D., Al-Saran, Y., Awlia, A., Abou-Rjeili, M., Ouellet, S., Akoury, E., Lemarié, C. A., Henderson, J. E., & Martineau, P. A. (2019). Defective bone repair in diclofenac treated C57Bl6 mice with and without lipopolysaccharide induced systemic inflammation. *Journal of Cellular Physiology*, *234*(3), 3078–3087. https://doi.org/10.1002/jcp.27128

Ramirez-GarciaLuna, J. L., Chan, D., Samberg, R., Abou-Rjeili, M., Wong, T. H., Li, A., Feyerabend, T. B., Rodewald, H.-R., Henderson, J. E., & Martineau, P. A. (2017). Defective bone repair in mast cell-deficient Cpa3Cre/+ mice. *PLoS One*, *12*(3), e0174396. https://doi.org/10.1371/journal.pone.0174396

Sanz, M., Dahlin, C., Apatzidou, D., Artzi, Z., Bozic, D., Calciolari, E., De Bruyn, H., Dommisch, H., Donos, N., Eickholz, P., Ellingsen, J. E., Haugen, H. J., Herrera, D., Lambert, F., Layrolle, P., Montero, E., Mustafa, K., Omar, O., & Schliephake, H. (2019). Biomaterials and regenerative technologies used in bone regeneration in the craniomaxillofacial region: Consensus report of group 2 of the 15th European workshop on periodontology on bone regeneration. *Journal of Clinical Periodontology*, *46*(S21), 82–91. https://doi.org/10.1111/jcpe.13123

Slichter, S. J., & Harker, L. A. (1976). Preparation and storage of platelet concentrates: I. Factors influencing the harvest of viable platelets from whole blood. *British Journal of Haematology*, *34*(3), 395–402. https://doi.org/10.1111/j.1365-2141.1976.tb03586.x

Steller, D., Herbst, N., Pries, R., Juhl, D., & Hakim, S. G. (2019). Positive impact of platelet-rich plasma and platelet-rich fibrin on viability, migration and proliferation of osteoblasts and fibroblasts treated with zoledronic acid. *Scientific Reports*, *9*(1), 8310–8310. https://doi.org/10.1038/s41598-019-43798-z

Stincone, A., Prigione, A., Cramer, T., Wamelink, M. M., Campbell, K., Cheung, E., Olin, M. V., Grüning, N.-M., Krüger, A., Alam, M. T., Keller, M. A., Breitenbach, M., Brindle, K. M., Rabinowitz, J. D., & Ralser, M. (2015). The return of metabolism: Biochemistry and physiology of the pentose phosphate pathway. *Biological Reviews of the Cambridge Philosophical Society*, *90*(3), 927–963. https://doi.org/10.1111/brv.12140

Varley, M. C., Neelakantan, S., Clyne, T. W., Dean, J., Brooks, R. A., & Markaki, A. E. (2016). Cell structure, stiffness and permeability of freeze-dried collagen scaffolds in dry and hydrated states. *Acta Biomaterialia*, *33*, 166–175. https://doi.org/10.1016/j.actbio.2016.01.041

Victoria, G., Petrisor, B., Drew, B., & Dick, D. (2009). Bone stimulation for fracture healing: What's all the fuss? *Indian Journal of Orthopaedics*, *43*(2), 117–120. https://doi.org/10.4103/0019-5413.50844

Vincent, E. E., Sergushichev, A., Griss, T., Gingras, M. C., Samborska, B., Ntimbane, T., Coelho, P. P., Blagih, J., Raissi, T. C., Choinière, L., Bridon, G., Loginicheva, E., Flynn, B. R., Thomas, E. C., Tavaré, J. M., Avizonis, D., Pause, A., Elder, D. J. E., Artyomov, M. N., & Jones, R. G. (2015). Mitochondrial phosphoenolpyruvate carboxykinase regulates metabolic adaptation and enables glucose-independent tumor growth. *Molecular Cell*, *60*(2), 195–207. https://doi.org/10.1016/j.molcel.2015.08.013

Yamamoto, M. K., D'Avila, R. P., & Luz, J. G. (2013). Evaluation of surgical retreatment of mandibular fractures. *Journal of Cranio-Maxillo-Facial Surgery*, *41*(1), 42–46. https://doi.org/10.1016/j.jcms.2012.05.008

Zhang, D., Wu, X., Chen, J., & Lin, K. (2018). The development of collagen based composite scaffolds for bone regeneration. *Bioactive Materials*, *3*(1), 129–138. https://doi.org/10.1016/j.bioactmat.2017.08.004

SUPPORTING INFORMATION

Additional supporting information may be found in the online version of the article at the publisher's website.

How to cite this article: Al-Hamed, F. S., Abu-Nada, L., Rodan, R., Sarrigiannidis, S., Ramirez-Garcialuna, J. L., Moussa, H., Elkashty, O., Gao, Q., Basiri, T., Baca, L., Torres, J., Rancan, L., Tran, S. D., Lordkipanidzé, M., Kaartinen, M., Badran, Z., & Tamimi, F. (2021). Differences in platelet-rich plasma composition influence bone healing. *Journal of Clinical Periodontology*, *48*(12), 1613–1623. https://doi.org/10.1111/jcpe.13546

1600051x, 2021, 12, Downloaded from https://onlinelibrary.wiley.com/doi/10.1111/jcpe.13546 by Spanish Cochrane National Provision (Ministerio de Sanidad), Wiley Online Library on [31/10/2023]. See the Terms and Conditions (https://onlinelibrary.wiley.com/terms-and-conditions) on Wiley Online Library for rules of use; OA articles are governed by the applicable Creative Commons License